A method for enlarging the Kerr constant of polymer-stabilised blue phases

Takashi Iwata[ab]; Ken Suzuki[a]; Hiroki Higuchi[c]; Hirotsugu Kikuchi[c]

[a] NOF Corporation, Tsukuba, Ibaraki, Japan [b] Department of Applied Science for Electronics and Materials, Kyushu University, Kasuga, Fukuoka, Japan [c] Institute for Material Chemistry and Engineering, Kyushu University, Kasuga, Fukuoka, Japan

PLEASE SCROLL DOWN FOR ARTICLE

Taylor & Francis
Taylor & Francis Group

A method for enlarging the Kerr constant of polymer-stabilised blue phases

Takashi Iwata[a,b], Ken Suzuki[a], Hiroki Higuchi[c] and Hirotsugu Kikuchi[c]*

[a]NOF Corporation, 5-10 Tokodai, Tsukuba, Ibaraki 300-2635, Japan; [b]Department of Applied Science for Electronics and Materials, Kyushu University, 6-1 Kasuga-koen, Kasuga, Fukuoka 816-8580, Japan; [c]Institute for Material Chemistry and Engineering, Kyushu University, 6-1 Kasuga-koen, Kasuga, Fukuoka 816-8580, Japan

Polymer-stabilised blue phase (PSBP) is one of the most promising materials for display devices because of its superior electro-optical properties compared with conventional nematics. However, the application of the PSBP has a serious practical issue in that the driving voltage required is too high to drive with thin film transitors, that is, the magnitude of the Kerr constant of PSBPs is insufficient. We present a useful method for increasing the Kerr constant based on the control of polymer aggregation structure using a cross-linker with a chiral structure. The director distortion arising from polymer networks in the PSBP seems to be responsible for the resulting improvement.

Keywords: Kerr effects; blue phase; polymer; birefringence

1. Introduction

Liquid crystal displays (LCDs) have become the leading technology for flat panel displays and are expected to continue to grow worldwide as a mainstream of TV. However, there remains a problem in displaying fast-moving images due to the slow response of nematic liquid crystals (LCs). The demand for LCDs with a fast response has been growing rapidly not only to improve the quality of the moving image but also to reduce the power consumption combined with the field sequential colour technology. Recently we proposed that the electro-optical Kerr effect of optically isotropic LCs has great potential for application in fast response LCDs, and we reported that polymer-stabilised blue phases (PSBPs) (*1*, *2*) and polymer-stabilised isotropic phases (*3*, *4*) showed an extraordinarily large Kerr constant. The Kerr law is generally given by (*5*):

$$\delta n = B\lambda E^2 \qquad (1)$$

where δn is electric field-induced birefringence, B is the Kerr constant, λ is the probe wavelength, and E is the electric field applied to the isotropic media. While the PSBP is a strong candidate for next-generation LCDs because of its fast response, the high driving voltage is a difficult problem to resolve in practical applications (*6*). In order to reduce the driving voltage of the Kerr effect, the magnitude of B needs to be enlarged. Therefore, there is an important challenge to develop a new PSBP material with a large Kerr constant. The Kerr constant B of a blue phase (BP) is reported to obey the following equation (*7*):

$$B \equiv \frac{\delta n}{E^2} = \Delta n \frac{\varepsilon_0 \Delta \varepsilon}{Kq^2} \qquad (2)$$

where Δn, $\Delta \varepsilon$ and K are the refractive index anisotropy, the dielectric anisotropy and the elastic constant of the LC materials, respectively. q is the elastic deformation wave number, which is in inverse proportion to the lattice constant a of a BP. a is related to the cholesteric pitch P_0 of LC materials, for example, a is nearly equal to P_0 in the case of BPI. Although to increase a is, therefore, an effective method for enlarging B and reducing the driving voltage, there is an upper limit to increasing a because a BP is coloured due to the Bragg diffraction of the visible wavelength, which leads to a lowering of the contrast ratio of a displaying image if a is larger than a certain value. Therefore, there is a crucial trade-off between the driving voltage and the contrast. Here we describe a method which provides the PSBP with a relatively large Kerr constant and a sufficiently small lattice constant at the same time.

2. Experimental

2.1 Sample preparation

Chemical structures of the material used in this work are given in Figure 1. We used photo-polymerisable chiral dopant 2, 5–bis-[4′-(3-(acryloyloxy)propyloxy)-phenyl-4-carbonyl]-1, 4; 3, 6-dianhydride-D-sorbitol (ISO(C3AcOBA)$_2$, synthesised by ourselves) as the chiral nematic (N*-LC) LC component. ISO(C3AcOBA)$_2$ induced cholesteric pitch to nematic LCs (*8*), in addition, after polymerisation, ISO(C3AcOBA)$_2$ was excreted from nematic media

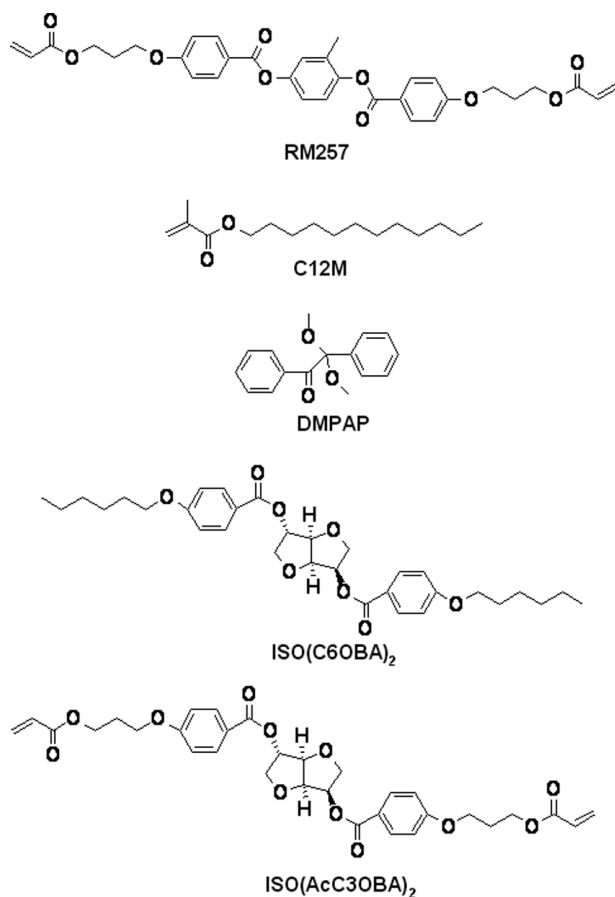*Corresponding author. Email: kikuchi@cm.kyushu-u.ac.jp

Figure 1. Chemical structure of sample components.

TCI, Tokyo, Japan), and cross-linker 2-methyl-1,4-phenylene-bis{4[3(acryloyloxy)propyloxy]benzoate} (RM257, Merck). These materials were homogeneously mixed in the weight ratio 92.0 (N*-LC mixture)/4.0(C12M)/4.0 (RM257). The composition of precursors was based on previous work (*1*, *2*). In order to initiate the polymerisation by UV light, 0.4 wt% of photoinitiator 2, 2-dimethoxy-2-phenylacetophenone (DMPAP, Aldrich) was added to the precursors. The precursors were irradiated with UV light from a metal halide lamp (SPOTCURE SP-V, Ushio, Cypress, CA, USA) for photopolymerisation, and the intensity and the exposure time of UV were 1.5 mW cm^{-2} at 365 nm and 40 minutes, respectively.

The phase behaviour of the precursors was characterised by observing the optical texture under a crossed polariser with a polarising optical microscope (OPTIPHOT2-POL, Nikon) equipped with a heating stage (LTS-E350, Linkum).

The heating and cooling of the samples were controlled at the rate of 1 K min^{-1}. The evaluated transition and polymerisation temperatures are shown in Table 2. Although samples 2 and 3 showed only BPI, all precursors showed BP in a similar temperature range.

The samples were loaded into the cells with a cell gap of $d = 10$ μm (maintained by a polyethylene terephthalate film spacer) in the isotropic state. The cell configuration is shown in a previous report (*4*), i.e. the interdigitated comb-like Cr electrodes were made on only one inner side of the glass substrate. The width of the comb plate was 5 μm and the distance between neighbouring plates was 10 μm.

2.2   *Reflection spectroscopy*

Reflection spectroscopy was performed to estimate the unit cell constant *a* of a BP. The reflection resulted from the Bragg diffraction of the cubic lattice of the BP, therefore *a* was calculated from the peak wavelength, λ_{peak}, of the measured reflection spectra. The measurements were carried out at the polymerisation temperature before and after polymerisation with a spectrophotometer (MSV-350, Jasco).

and cholesteric pitches vanished if no other chiral dopant was added to the host LCs (see supplementary material which is available via the multimedia link on the online article webpage). Other N*-LC LC components included the nematic LC 4-cyano-4′-pentylbiphenyl (5CB, Aldrich), fluorinated nematic mixture JC1041xx (Chisso, Tokyo, Japan) and another chiral dopant, 2, 5-bis-[4′-(hexyloxy)-phenyl-4-carbonyl]-1, 4; 3, 6-dianhydride -D-sorbitol (ISO(C6OBA)$_2$, synthesised by ourselves.

The constituent fractions of the N*-LC mixtures are shown in Table 1. The precursors consisted of the N*-LC mixture, *n*-dodecyl methacrylate (C12M,

Table 1. Composition of N*-LC mixtures.

Molar ratio /wt%	No.	Liquid crystal		Chiral dopant	
		JC1041XX	5CB	ISO(C6OBA)$_2$	ISO(C3AcOBA)$_2$
	1	45	45	5	5
	2	47	47	6	0
	3	46.75	46.75	6.5	0
	4	46.5	46.5	7	0
	5	46.25	46.25	7.5	0

Table 2. Phase transition and polymerisation temperature of monomer/LC samples.

No.	N*		BPI		BPII		Iso	Polymerisation temperature/K
			Phase transition temperature/K					
1	·	301.3	·	302.6	·	303.6	·	302.5
2	·	310.4	·	-		312.5	·	310.5
3	·	309.9	·	-		312.0	·	311.0
4	·	308.6	·	309.5	·	310.5	·	309.0
5	·	307.9	·	308.7	·	309.4	·	308.5

2.3 Electro-optical properties

The electro-optical properties of the PSBP were measured by a popular system for sandwiched cells (see supplementary material which is available via the multimedia link on the online article webpage). In order to calculate the transmittance T, the transmitted light intensity of sample cells at isotropic state under parallel Nicoles was set to $T = 100\%$ and the light intensity of crossed Nicoles set to $T = 0\%$. All electro-optical measurements were carried out at 298 K.

3. Results and discussion

Figure 2 shows the typical reflection spectra and polarising micrographs obtained for sample 4 before and after polymer-stabilising BP by *in situ* photopolymerisation. The reflection peak caused by Bragg diffraction from the BP lattice was retained after polymerisation, while the peak wavelength shifted to a longer wavelength and the peak width broadened after polymerisation. The colours observed by
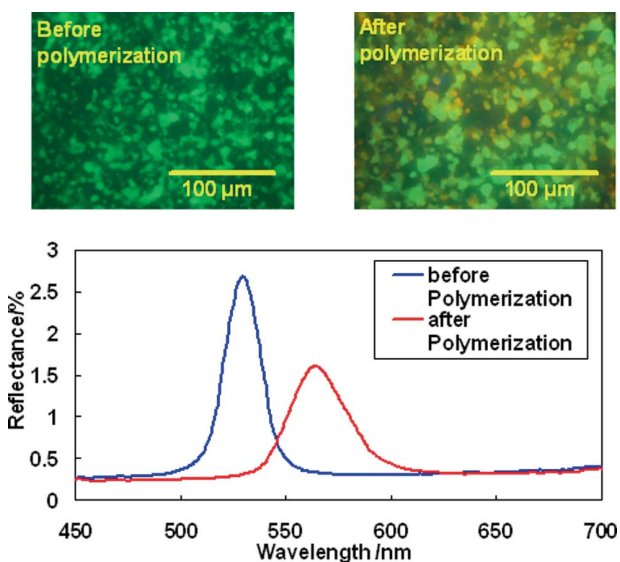
polarising optical microscopy were identical with the reflection spectra and these results were common to all samples. Although the reason why the red shift occurred has not become clear yet, a possible reason is that the helical pitches or refractive indices of the BP were varied because the compositions of monomer/LC mixtures should change with progressing polymerisation.

In general the Bragg diffractions of the bcc lattice of BPI occurs from the planes of {110}, {220}, {211}, in order from the long wavelength (*9*). The diffraction from {220} appears near the wavelength of the selective reflection of the N* phase, which is a lower temperature phase of BP. Figure 3 shows reflection spectra and polarising micrographs obtained for samples 1–5 before polymerisation. The magnitudes of the reflectance are normalised by the maximum value of each corresponding peak. The observed peaks in the visible wavelength region are reasonably assigned to Bragg diffraction from the {110} plane of the bcc lattice of BPI because the observed wavelength was roughly 1.4 times larger than that of the selective reflection of the corresponding N*.

Figure 4 shows normalised reflection spectra and polarising micrographs obtained for samples 1–5 after

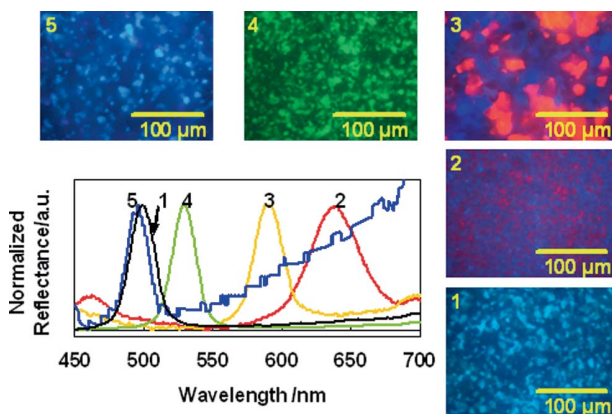Figure 2. Typical reflection spectra and polarising micrographs obtained for sample 4.

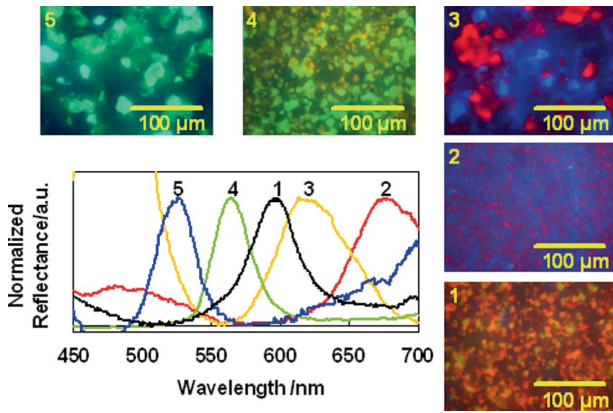Figure 3. Normalised reflection spectra and optical micrographs for various samples before polymerisation.

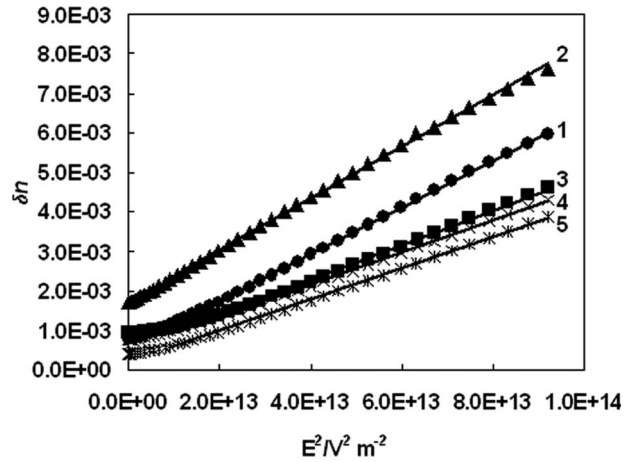Figure 4. Normalised reflection spectra and optical micrographs for various samples after polymerisation.

Figure 5. The field-induced birefringence plotted against the electric field squared for various samples. Solid lines are approximations.

polymerisation. The same tendency of chirality dependence shown in Figure 3 was also observed in Figure 4, while the peak shift of sample 1 due to polymerisation was larger than those of samples 2–5, indicating that the lattice size of sample 1 increased after polymerisation.

During polymerisation, the produced polymers segregate from the low molecular weight LCs and a phase separation occurs at sub-micrometre level (*10*). If the precursor includes a polymerisable chiral dopant like sample 1, the chirality should reduce after polymerisation because the concentration of the chiral dopant decreases within the LC region by segregating the polymerisable monomers to be confined in the polymer. However, the resulted reflection peak wavelength of sample 1 was shorter than those of samples 2 and 3, which contain more non-polymerisable chiral dopant $ISO(C6OBA)_2$ than sample 1. It is conceivable that sample 1 has a smaller unit cell length a than in samples 2 and 3.

Electric field-induced birefringence was calculated from the measured transmittance T using the following equation in the range of $\pi\delta nd < \lambda$:

$$T = \sin^2 \frac{\pi\delta nd}{A\lambda} \qquad (3)$$

where d and λ were the cell gap and probe wavelength, respectively. A is the correction factor of the Kerr constant B. Though the electric field is applied normal to the cell gap direction and the electric flux density is not uniform throughout the In-Plane-Switching cell, the estimated Kerr constants B using the IPS cell become smaller in value compared with the true values. The value of A is 4.57 in our experimental conditions.

Figure 5 shows the plots of the electric field-induced birefringence for samples 1–5 after

polymerisation. Due to the optical leakages resulting from Bragg diffraction or light scattering, the induced birefringence of the off-state was not completely zero. Optical leakage of the off-state was smallest for sample 5. This might be because the wavelength of the Bragg diffraction peak was furthest from the probe wavelength, 633 nm. Sample 2 showed the largest optical leakage, the reflectance peak was farther from the probe wavelength compared with sample 3. We think that the BP was not perfectly stabilised in sample 2, which showed N* partly having a large birefringence. The electric field-induced birefringence was clearly proportional to the square of the applied electric field if the optical leakage was subtracted, indicating that the Kerr law was satisfied. The Kerr constant B was calculated from the slope of the electric field-induced birefringence as a function of the square of the electric field E. Figure 6 shows the plots of the reflection peak wavelengths dependence on B of samples 1–5.
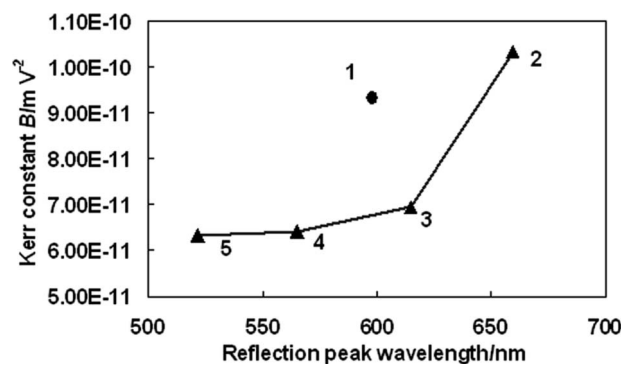

Figure 6. The variation of Kerr constants B with reflection peak wavelengths.

The magnitudes of *B* for samples 2–5 increased with increasing the reflectance peak wavelength, which is related to the lattice parameter of BP. This trend is in agreement with Equation (2). On the other hand, the magnitude of *B* of sample 1 deviated clearly from this trend to a larger value. Generally the lattice parameter of BP is determined mainly by the helical pitch, $a \sim p$ in the case of BPI. The polymer produced by *in situ* polymerisation in the BP is supposed to fix the lattice parameter of the BP. If a part of the chiral dopants is a polymerisable monomer like sample 1, the initial equilibrium helical pitch and the final one should be different because the concentration of chiral dopant within the LC phase changes as the polymerisation progresses. Since the fixation of the BP lattice progresses at the same time, the fixed lattice parameter and the equilibrium helical pitch should be different. The concentration of chiral dopant is reduced during polymerisation in the case of sample 1. Therefore, the resulting helical pitch should obviously be smaller than the equilibrium helical pitch; in other words, the twisted structure of the molecules is elastically distorted for sample 1. The important point to note is that this situation affects the mobility of LC molecular realignment by an external field. Considering an electric response of a twisted nematic (TN) cell, for example, when the twisting ratio of the director imposed by the interfaces with the substrates is larger than the equilibrium twisting ratio without any substrate, the threshold voltage to drive a TN cell decreases compared with when both ratios are identical. Thus it is reasonable to conclude that the exceptionally large Kerr effect of sample 1 is due to a stored elastic distortion resulting from the imposed smaller helical pitch than the equilibrium value without polymers. We believe that these results will lead to a new method of lowering the driving voltage of PSBP electro-optical devices.

4.   Conclusions

We proposed a method for giving a larger Kerr constant to PSBP by polymerisation-induced director distortions. Such an effect can be explained on the basis of the analogy of TN systems.

Acknowledgements

References

(1) Kikuchi, H.; Yokota, M.; Hisakado, Y.; Yang, H.; Kajiyama, T. *Nat. Mater.* **2002**, *1*, 64–68.
(2) Hisakado, Y.; Kikuchi, H.; Nagamura, T.; Kajiyama, T. *Adv. Mater.* **2005**, *17*, 96–98.
(3) Haseba, Y.; Kikuchi, H.; Nagamura, T.; Kajiyama, T. *Adv. Mater.* **2005**, *17*, 2311–2315.
(4) Choi, S-W.; Yamamoto, S.; Haseba, Y.; Higuchi, H; Kikuchi, H. *Appl. Phys. Lett.* **2008**, *92*, 043119.
(5) Kerr, J. *Philos. Mag.* **1875**, *50*, 337–348.
(6) Yoneya, M.; Takada, S.; Maeda, Y.; Yokoyama, H. *Liq. Cryst.* **2008**, *35*, 339–342.
(7) Gerber, P.R. *Mol. Cryst. Liq. Cryst.* **1985**, *116*, 197–206.
(8) Hoischen, A.; Kitzerow, H.-S.; Kűrschner, K.; Strohriegl, P. *J. Appl. Phys.* **2000**, *87*, 2105–2109.
(9) Wright, D.C.; Mermin, N.D. *Phys. Rev. A* **1985**, *31*, 3498–3500.
(10) Iwata, T.; Suzuki, K.; Amaya, N.; Higuchi, H.; Masunaga, H.; Sasaki, S.; Kikuchi, H. *Macromolecules.* **2009**, *42*, 2002–2008.